PROPELLER PERFORMANCE MEASUREMENT FOR LOW REYNOLDS NUMBER UNMANNED AERIAL VEHICLE APPLICATIONS

A Thesis by

Monal Pankaj Merchant

B.S., Wichita State University, 2004

Submitted to the College of Engineering
and the faculty of the Graduate School of
Wichita State University
in partial fulfillment of
the requirement for the degree of
Master of Science

December 2005

PROPELLER PERFORMANCE MEASUREMENT FOR LOW REYNOLDS

NUMBER UNMANNED AERIAL VEHICLE APPLICATIONS

I have examined the final copy of this thesis for form and content and recommend that it be accepted in partial fulfillment of the requirements for the degree of Master of Science with a major in Aerospace Engineering

_____
Dr. L. Scott Miller, Committee Chair

We have read this thesis
And recommend its acceptance:

_____
Dr. Klaus A. Hoffmann, Committee Member

_____
Dr. David N. Koert, Committee Member

DEDICATION

To Mum and Dad:

For their constant support, help and understanding

Determination, Dedication, Devotion and Discipline are the four necessary ingredients for success…

ACKNOWLEDGEMENTS

I thank the department of Aerospace Engineering, Wichita State University, for their support. I would specially like to acknowledge the help extended by Philip Butler and Joshua Nelson, in and towards this effort. Last, but not least, a special thanks to my supervisor, advisor and mentor, Dr. L. Scott Miller for all his support, advice and encouragement throughout my undergraduate and graduate years; I do not have enough words to thank you!

ABSTRACT

The recent increase in the development of UAV's and MAV's has created a strong demand for small propeller performance data. Propeller performance is critical to the success of these aircraft and guaranteed performance demands accurate experimental data. These propellers operate at low Reynolds numbers (between 30,000 and 300,000), rendering performance scaling from larger counterparts inaccurate. An Integrated Propulsion Test System has been designed, developed and validated at Wichita State University to accurately and reliably measure performance of small propellers. Performance of a large number of propellers has been charted and a database of performance data has been created. This thesis discusses the salient features of this measurement system and data for a few of the, over 30 propellers, charted.

TABLE OF CONTENTS

LIST OF TABLES

LIST OF FIGURES

LIST OF SYMBOLS

Symbol		Equation	Unit
α	Angle of Attack		degree
A2D	Analog-to-Digital		
AIAA	American Institute of Aeronautics and Astronautics		
A_P	Propeller disc area		ft^2
β	Yaw angle		degree
C	Jet cross-section area		ft^2
$C_{0.75}$	Blade Chord Length (75% radius location)		ft
C_P	Power Coefficient	$C_P = \frac{P_p}{\rho \cdot n^3 \cdot D^5}$	
C_Q	Torque Coefficient	$C_Q = \frac{Q}{\rho \cdot n^2 \cdot D^5}$	
C_T	Thrust Coefficient	$C_T = \frac{T}{\rho \cdot n^2 \cdot D^4}$	
D	Propeller Diameter		ft
DC	Direct Current		
η_P	Propeller Efficiency	$\eta_p = J \cdot \frac{C_T}{C_P}$	
i	Current in amperes		a
J	Advance Ratio	$J = \frac{U'}{n \cdot D}$	
MAV	Micro Air Vehicle		
n	Revolutions Per Second	$n = \frac{RPM}{60}$	
p	Pressure (Atmospheric)		lb/ft^2

P_P	Propeller Power output	$P_p = \Omega \cdot Q$	Watt
Q	Dynamic Pressure (Tunnel)		lb/ft^2
Q	Torque		ft-lb
ρ	Density		$slug/ft^3$
R	Gas Constant		
R/C	Radio Control		
$Re_{0.75}$	Reynolds Number (Refered to blade chord at 75% radius)	$\mathrm{Re}_{0.75} = \frac{\rho \cdot U_t \cdot C_{0.75}}{\mu}$	
RPM	Revolutions Per Minute		
T	Thrust		lb
T_t	Temperature		°R
U	Uncorrected Velocity		ft/s
U'	Corrected Velocity	$U' = U \cdot \left(1 - \frac{\tau_4 \cdot \alpha_1}{2 \cdot \sqrt{1 + 2 \cdot \tau_4}}\right)$	ft/s
U_t	Tangential Velocity		ft/s
UAV	Unmanned Aerial Vehicle		
v	Volt		v
Ω	Radians per Second		
WOZ	Wind-Off Zero		
WSU	Wichita State University		

CHAPTER 1

1.0 INTRODUCTION

1.1 General Background

The development of Unmanned Aerial Vehicles (UAV's) and interest in Micro Aerial Vehicles (MAV's) has increased over the last decade. These few years have also witnessed an ever-increasing number of radio controlled (R/C) airplane hobbyists and amateur R/C airplane designers. The hobby of flying R/C airplanes is slowly turning into a professional sport with the increasing number of competitions not only encouraging the hobbyist to modify off-the-shelf scale designs but also stimulating interest amongst engineering students in universities, challenging them to design mission specific R/C aircrafts.

Performance data for a large number of propellers, used in conventional sized aircraft has been charted and cataloged. This helps engineers select the appropriate propeller for a given aircraft or optimize a current propeller design to suite a specific mission requirement. The smallest propellers previously charted are generally close to four feet in diameter, operate at high RPM, and relatively high forward speeds, thereby high operating Reynolds numbers. Unlike these, the propellers used for UAV's, MAV's or model R/C aircrafts, are generally of diameters less than two feet. Although they may operate at relatively high RPM, their operating Reynolds numbers are very low, normally less than 300,000, primarily due to small chord lengths and relatively low forward speeds. Since the operating Reynolds number affects the magnitude of drag due to skin friction and

separation, small propellers performance results being different from their larger counterparts.

The extent of accurate and reliable testing that has been done on these small propellers is practically non-existent compared to the large, full scale propellers. And, even if tests have been carried out, no systematic documentation exists in the public domain, proving to be a major handicap for UAV, MAV or model R/C aircraft designers and engineers.

1.2 Importance of Propeller Performance Data

The importance of propeller performance data can be directly co-related to airfoil data and its importance in aircraft design. Verification of aircraft performance demands accurate experimental results, be it airfoil data, propeller performance data or an entire wind tunnel test. The propulsion system directly contributes to the success of mission specific airplanes, be it mere pylon racing, surveillance, atmospheric research or communication relays. Since propeller selection is critical to a good propulsion system, thus the availability of propeller performance data is as critical to a successful design.

1.3 Existing Problems

The propellers considered under Small Propellers, typically operate at Reynolds numbers between 30,000 to 300,000 (based on chord at ¾ radius and sea level conditions) and the low Reynolds number effects start prominently showing up with decreasing Reynolds number.

As an aid to the designer, most engine manufacturers [1] recommend a propeller pitch and diameter combination that could be used with their engines. But, no supporting performance or test data is made available to the end user thereby placing the assumptions validity into question.

Now, with this resource, or the lack of it, dismissed, one can attempt and use computational tools to predict the prospective propellers performance using theoretical and analytical schemes such as Vortex method, Blade Element Theory, Momentum Theory or a combination thereof [2]. The only limitation here is that off-the-shelf commercially available propellers may not be easy to model. In order to be fairly accurate, programs based on these theories need accurate airfoil data. Most of these propellers do not use any specific airfoil as such. A larger variety of the wooden propellers have a flat bottom, cambered top cross-section, while other propellers may use a combination of modified airfoils [3]. In any case, this data is not made available to the end user, thus limiting the accuracy with which this may be achieved and thus establishing a requirement for the existence of a standard experimental propeller performance database.

Although, work in this direction has been previously attempted [4 – 6], its progress has been very limited, primarily due to the lack of accuracy in measurement system. In some cases, when the measurement systems have had acceptable sensitiveness, they have experienced structural limitations due to vibration [6], [7]. Some efforts that have concentrated on wind tunnel testing of scaled propellers have used complex systems with propeller diameters although small, but much larger than the ones being considered here [5], [8]. They too,

have acknowledged the difficulties faced when entering the Reynolds number regimes considered here.

Lastly, measurement systems used for marine propellers of similar diameter have existed [9], but their adaptation to aircraft propellers has not been successfully carried out, primarily due to the lack of system sensitivity.

1.4 Goals

The growing development in UAV's, MAV's scaled and R/C airplanes translate to extensive use of scaled or small diameter propellers and therefore, creates a strong demand for the availability of crucial propeller performance data.

This reason and the other shortcomings mentioned above, have served as the motivation to design and develop an accurate measurement system, that is sufficiently sensitive, highly repeatable and caters to propeller performance measurements for diameter ranges from 6 inches to 22 inches, operating in the 30,000 to 300,000 Reynolds number regime, and create a reliable propeller performance database to serve as an aid to designers and hobbyists for propeller selection.

A measurement system, using precision components has been designed, developed and tested at Wichita State University. This thesis discusses the measurement system's traits and salient features, its design, testing, results obtained and some interesting observations that were made in this process.

CHAPTER 2

2.0 EXPERIMENTAL APPARATUS

Integrated Propulsion Test System

2.1 Measurement System Overview

The measurement system developed here can be divided into three sub-systems, namely, the Propeller Balance (sensor platform), Signal Conditioners and the Data Acquisition system (signal processing). Each sub-system comprises of electronic instrumentation and components as shown in the schematic in Figure 1, and is discussed below.

The propeller balance fixture is located inside the 3’ x 4’ wind tunnels test section. It includes the wind tunnel C-strut, the balance mount and balance, a multi-motor adapter, an electric motor, the RPM sensor, tunnel air data sensor and the propeller. This connects to the Signal Conditioners, external to the wind tunnel test section. The Signal Conditioners comprise of power supplies, terminal box, multi-module signal amplifier and an array of optical isolators. Lastly, signal processing is accomplished by the Data Acquisition and Reduction sub-system. This sub-system encompasses a screw terminal, the A2D card, the computer and software.

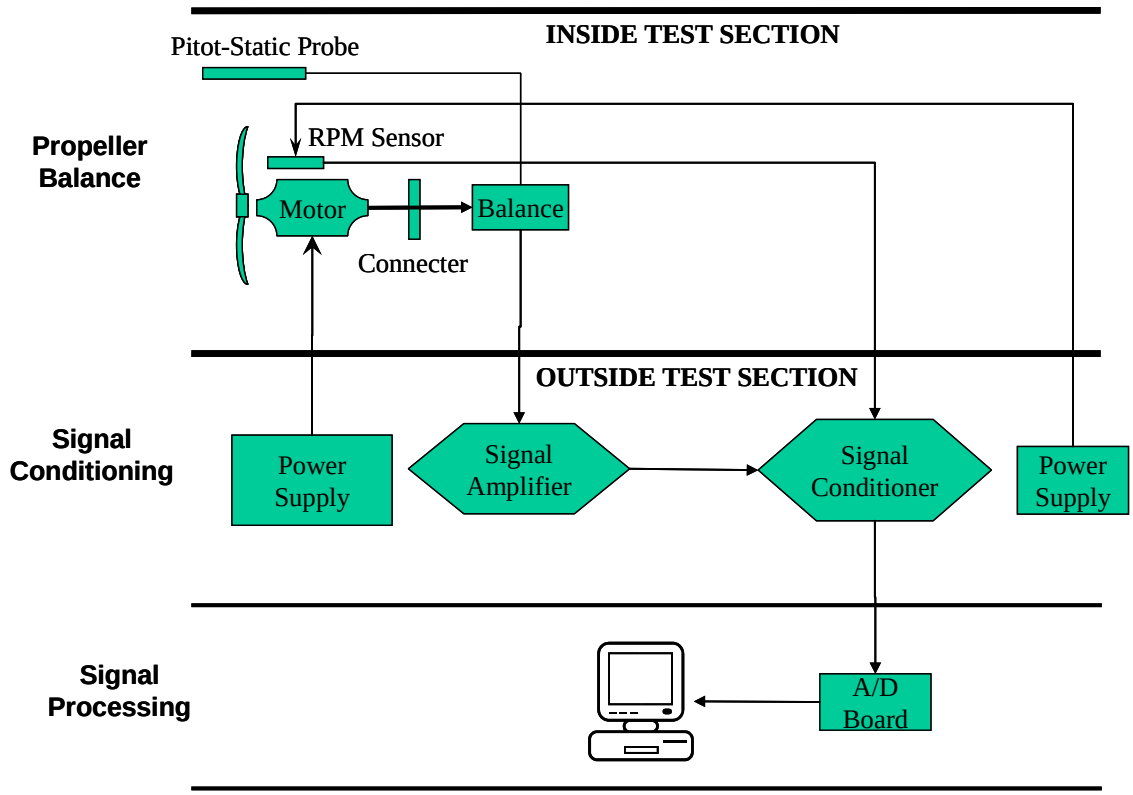

Figure 1: IPTS Schematic overview

2.2 Propeller Balance Fixture

The main sensors here are mounted on and supported by the C-strut and a solid steel adapter, giving the entire fixture a firm foundation. A two-component load cell made by FUTEK, and capable of accurately measuring thrust and torque loads, is mounted on this steel adapter. This load cell is capable of measuring up to 50 lb in thrust and 50 in-lb in torque, with a rated output accuracy of 0.05% FS (full scale).

The multi-motor adapter is mounted on the load cell. As described by its name, this adapter is designed to accommodate a large range of motors. This increases the usable range of propeller diameters for this system. The motor is

mounted on this adapter. To date, three motors, all belonging to the Astroflight Cobalt motor family [1] have been used with this system.

The propeller RPM is measured by a Dynapar Series 54ZT Magnetic Pickup. The pickup is capable of measuring a maximum of 20,000 targets/s. This unit requires a magnetic target to be placed within 0.03 inches, in order to record its pass. This is accomplished by placing a steel tab behind the propeller near the hub. The output from this is a square waveform, which is converted to RPM readout through the data acquisition program which is discussed in detail in the following sections.

The wind tunnel's dynamic pressure or Tunnel q, is measured using a pitot-static probe, which is connected to a high precision 1-psid Honeywell Precision Transducer, rated at 0.05% FS accuracy. The signal output from this transducer along with outputs from all the other sensors mentioned here, are processed through the Signal Conditioners, described below.

2.3 Signal Conditioners

The signal conditioning sub-system is located outside the wind tunnel test section, but within three feet of all the sensors, so as to maintain the signal quality. A home-built enclosed screw terminal serves as a hub to segregate power and signal wires and connect them to the respective amplifiers.

Signal amplification and partial signal conditioning is accomplished using a multi-module Vishay-Ellis 2210 strain-gauge amplifier. This unit provides a very precise gain and filter setting and a hassle free signal zeroing. Post amplification,

the partially conditioned signals are processed through an array of Pepperl-Fuchs KFDX-DCV optical signal isolators. Thus, eliminating ground loops from the signals before they are processed by the Data acquisition and reduction sub-system.

Power to the motor and the RPM sensor is provided by two independent DC power supplies. A generic 15 volt power supply powers the RPM sensor, while a precision High wattage HP6032A Power Supply is used to precisely control power to the motor.

2.4 Data Acquisition and Reduction

Data acquisition is accomplished using a 16-bit Measurement Computing 16/16 DAS A2D PC Card in conjunction with a Pentium-4 laptop. The data is collected and reduced using a self-authored visual basic program that writes the data directly to an excel spreadsheet. This program automates the data reduction and archiving process and is capable of configuring the A2D board. The data reduction routine applies calibrations and accounts for propeller blockage corrections due to the spinning propeller in a closed throat wind tunnel. Non-dimentionalized propeller performance plots and a summarized performance tables are automatically generated and archived by this program.

2.5 The Facility

The 3 ft x 4 ft Low Speed Wind Tunnel (Figure 2) at Wichita State University is an open return wind tunnel with a 3 ft x 4 ft test section. The tunnel is equipped for force and pressure measurements and is capable of achieving speeds up to 180 ft/s.

Figure 2: The 3'x4' Low Speed Wind Tunnel, WSU

2.6 Propeller Selection

The ability of this system to accommodate multiple motors, allows a large diameter range of propellers that can be tested. To date the propellers selection has been based on specific test requirements, described in the following sections, and to encompass the general range of diameters, for demonstration purposes.

Although any propellers within the diameter range from 6 inches to 22 inches can be tested, the propellers that have been tested (Figure 3) so far were selected to cover a wide range of diameter, pitch and type. The selection and classification is described in the following sections.

Figure 3: Sample propellers

2.6.1 A Brief Note on Propeller Nomenclature

The nomenclature for propellers used in this thesis is consistent with the standard nomenclature [10] as used by model airplane propeller manufacturers.

The propeller name generally has a string of number with a dash or an x separating it from another number. The first number after the propeller company name indicates the propeller diameter in inches. The second number that follows is separated by either a '– 'or 'x 'indicates the propeller pitch in inches [11].

The pitch, here, is defined as the distance in inches a propeller would travel in one revolution. Any letters that follows this string of numbers is a code signifying the particular propellers specialty. For example,

Zinger 22 – 8 describes the propeller to have a 22 inch diameter and 8 inch pitch. And APC12 – 12 E describes the propeller to have a 12 inch diameter with a 12 inch pitch, and the letter E is a code classifying the propeller specially designed to be used with electric motors [3].

It is recommended that the user refer to the manufacturer's documentation to interpret this last letter.

CHAPTER 3

3.0 EXPERIMENTAL PROCEDURE

3.1 Test Procedure

During the design phase of the experiment, it was found that either the RPM or the forward velocity, or both needed to be varied, to vary the advance ratio in order to map the complete performance curves. Although various combinations of RPM and velocity were tried, varying the tunnel-q was found most effective and this procedure was also similar to the flight settings on a typical R/C airplane, i.e. most R/C airplanes are generally flown at full throttle settings. Thus, it was deemed important to select the tunnel-q step sizes in a manner that not only covered primarily the propeller efficiency curves entire regime for the entire range of propellers considered here, but also ensured that the resolution was varied in an appropriate manner. A program based on Combined Blade Element and Momentum Theory [2] was written for this purpose and used to select the required tunnel-q step sizes.

In the above process, the motor is operated at constant power (maximum power) at various tunnel speeds. This power is limited by the maximum continuous operation current and voltage specified by the motor manufacturer [1]. This limit is easily enforced by setting the ‘never exceed’ limits on current and voltage outputs on the power supply.

WOZ readings are taken during the start and end of each run and the average WOZ values are tared from the collected data.

The procedure for collecting data begins with executing the data acquisition and reduction program. The signal conditioning equipment is zeroed and WOZ readings taken. This is followed by powering the motor to conditions mentioned above and collecting data for each pre-determined ‘q’ step. Once the data is collected, the data reduction sub-routine is executed. The collected data is then systematically reduced, recorded, plotted and archived.

Due to complete automation of this process, the overall time required for an entire run is just the physical tunnel run time.

3.2 Uncertainty and Sensitivity Analysis

Sensitivity and uncertainty analysis [12], [13] were performed prior to the experimental setup and throughout the apparatus development. The Kline-McClintok [12] method has been used to perform uncertainty analysis on all variables.

The Kline-McClintok method is based on careful specification of uncertainties in various primary experimental measurements. Uncertainties of the measured variables are taken and used to compute the uncertainties in the calculated result using Equation 3.2.1 [13], where R is the result, w_R is the uncertainty in the result, x_n are the dependant variables and w_n are the uncertainties associated to those dependant variables.

$$w_R = \left[\left(\frac{\partial R}{\partial x_1} w_1 \right)^2 + \left(\frac{\partial R}{\partial x_2} w_2 \right)^2 + \ldots + \left(\frac{\partial R}{\partial x_n} w_n \right)^2 \right]^{1/2} \qquad (3.2.1)$$

The instrument accuracy, as stated in the documents provided by the respective manufacturers is given in Table 1. For all the other non-dimensional performance parameters, since their quantified accuracy depends on each individual data point, their typical values have been provided in the following section.

TABLE 1: INSTRUMENTATION ACCURACIES AT A GLANCE

Instrument	Measured Quantity	Unit	Accuracy (Rated Output)
Load Cell	Thrust	lb	±0.05%
	Torque	In-lb	±0.05%
Pressure Transducer	Test section Dynamic Pressure	lb/ft^2	±0.05%
Magnetic Pickup	RPM	RPM	±0.001% (Based on Algorithm)

Experimental apparatus sensitivity has also been tested by performing α and β sweep of ±3°. This helped determine the apparatus sensitivity to the propeller disc plane orientation. These results are further discussed in the results and discussion section.

3.3 System Calibration

Before using the IPTS for any tests, each measuring instrument has been calibrated.

The Load cell is calibrated insitu, using calibrated weights. A special calibration apparatus, shown in Figure 4, that applies pure thrust and torque loads, was specially designed for this purpose.

Figure 4: IPTS Torque and Thrust calibration

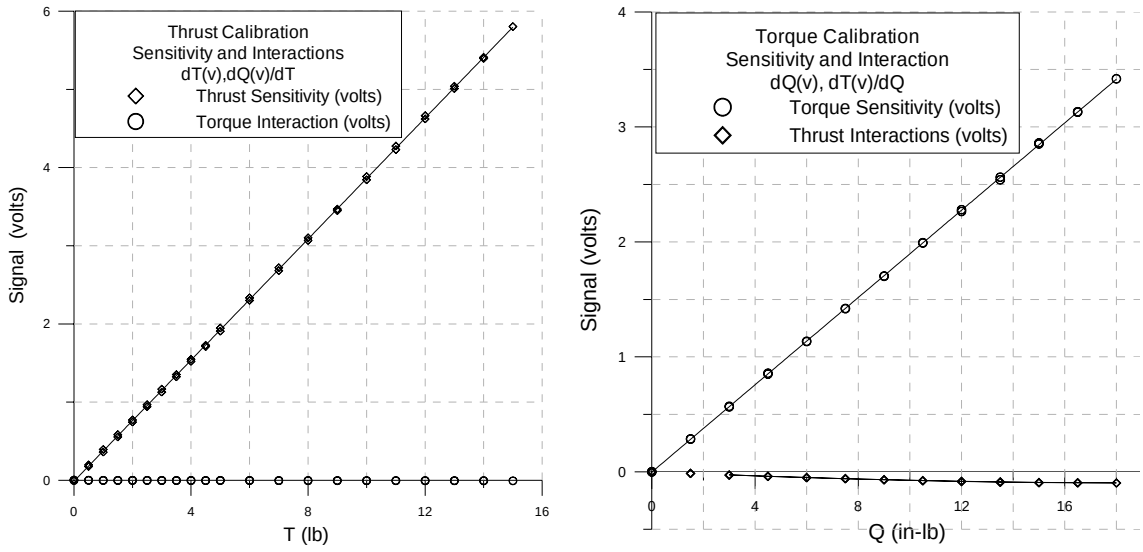

Figure 5: IPTS calibration plots

Calibration is later verified using check-loads. Pure and combined check loads are repeatedly applied to verify balance calibration. The balance behavior is found to be very linear in sensitivities and minimal interactions are observed due to each channel, as can be seen in Figure 5. These are accounted for in the final balance behavior matrix [14].

Although the RPM indicator does not need any calibration, its readings are verified using a calibrated strobe light and are further examined by measuring the frequency using a multimeter. The algorithm developed for the purpose of measuring the magnetic pickups signal and converting them to RPM, has also been checked against the multimeter for flawless operation.

The algorithm, described in the following section, is a simple formulation that counts the number of positive slopes that occur in the magnetic pickup signal over the sample period, average them over a second and convert them to RPM.

The tunnel's dynamic pressure measurement transducer has been calibrated using a manometer. The calibration constant obtained matched the previous values used in the tunnel constants.

3.4 Variables and Performance Parameters

As mentioned previously, variables were divided into two categories, namely measured variables and calculated variables. The measured variables, are the dimensionalized variables that are directly measured from the various instruments. For calculating the non-dimensionalized performance parameters [15], more variables, dependant on the measured variables have been

calculated, and have thus been classified here as calculated variables. The measured variables along with their units have been shown in Table 2 below.

TABLE 2: TABLE OF MEASURED VARIABLES WITH UNITS

Measured Variables			
Quantity	*Source*	*Variable*	*Units*
Thrust	Load Cell	T	lb
Torque	Load Cell	Q	in-lb
Revolutions per minute	Magnetic pickup	RPM	RPM
Tunnel dynamic pressure	Pressure transducer	q	lb/ft^2
Voltage	Power supply	v	volt
Current	Power supply	i	ampere
Atmospheric Pressure	Weather services	p	in-Hg

For the ‘Calculated Variables’ a simple rearrangement of standard equations is performed to determine these variables. Conversion of RPM to revolutions per second RPS is required for the variable ‘n’ which is used in calculating performance parameters, and is calculated using Equation 3.4.1.

$$n = \frac{RPM}{60} \tag{3.4.1}$$

The uncorrected velocity “U”, with units in ft/s is calculated by rearranging the equation for dynamic pressure as show in Equation 3.4.2.

$$U = \sqrt{\frac{2 \cdot q}{\rho}} \tag{3.4.2}$$

The method and equation used to determine the corrected velocity “U” is given by Equation 3.5.1 and the method is described in the following section.

The power produced by the propeller P_p, with units in watts (Equation 3.4.3), is calculated using the equation given by Seddon [2], where Ω is in radians per second.

$$P_p = \Omega \cdot Q \text{ or } P_p = \left(RPM \cdot \frac{2\pi}{60} \right) \cdot \left(\frac{Q}{12} \right) \tag{3.4.3}$$

And finally, the last variable belonging to the ‘Calculated Variables’ class, density ‘ρ’, with units in slugs/ft^3, has been calculated by rearranging the standard pressure equality as shown in Equation 3.4.4, where pressure is in lb/ft^2, R is the gas constant and temperature ‘T_t’ is in degree-Rankin.

$$\rho = \frac{p}{R \cdot T_t} \tag{3.4.4}$$

Standard propulsion equations have been used to calculate non-dimensionalized performance parameters. Amongst these are coefficients for thrust (3.4.5), torque (3.4.6), power (3.4.7) and the propeller efficiency (3.4.8). Forward velocity, propeller RPM and diameter were combined into Advance

Ratio parameter (3.4.9). And, due to the nature of experiments, the Reynolds number (3.4.10) at 3/4th radius location was also calculated for each datapoint.

$$C_T = \frac{T}{\rho \cdot n^2 \cdot D^4} \tag{3.4.5}$$

$$C_Q = \frac{Q}{\rho \cdot n^2 \cdot D^5} \tag{3.4.6}$$

$$C_P = \frac{P_p}{\rho \cdot n^3 \cdot D^5} \tag{3.4.7}$$

$$\eta_p = J \cdot \frac{C_T}{C_P} \text{ or } \eta_p = \frac{\tau \cdot U'}{P_p} \tag{3.4.8}$$

$$J = \frac{U'}{n \cdot D} \tag{3.4.9}$$

$$\mathrm{Re}_{0.75} = \frac{\rho \cdot U_t \cdot C_{0.75}}{\mu} \tag{3.4.10}$$

3.5 Data Acquisition and Reduction System

The data acquisition and reduction program are written in Visual Basic for Applications (VBA) language, and embedded into MS Excel. The data acquisition program conFigures the A2D card and directly writes the output, as raw voltages, to the opened excel sheet.

The A2D card configuration, although optional, is preset for a sample rate of 5,000 Hz per channel with a sample period of 8 s. These values are based on the sensitivity studies performed for magnetic pickup and the load cell. The program uses these pre-set values, but also provides the user the option for changing them before initiating data acquisition.

The data reduction routine calculates the averages for all the signals, and converts them into respective engineering units. A special algorithm has been developed and is used to calculate propeller RPM form the magnetic pickup voltage readouts.

The program requires the user to input some basic information with regards to the propeller geometry, ambient temperature and temperature data, and the necessary file paths.

Other corrections that are required due to testing in the wind tunnel environment, such as solid blockage [14] and, especially for this experiment, propeller blockage corrections [14], [16] have been considered. Since uncertainty due to solid blockage is less than 0.3% for all cases, it has been ignored. On the other hand, since we are testing propellers in a closed-throat wind tunnel, propeller blockage corrections, or corrections due to the continuity effect, as described by Glauert [16], have been incorporated into the program. The correction for velocity is as given by Equation 3.5.1.

$$U' = U \cdot \left(1 - \frac{\tau_4 \cdot \alpha_1}{2 \cdot \sqrt{1 + 2 \cdot \tau_4}} \right) \tag{3.5.1}$$

where,

$$\tau_4 = \frac{T}{\rho \cdot A_P \cdot U^2} \tag{3.5.2}$$

$$\alpha_1 = \frac{A_P}{C} \tag{3.5.3}$$

Although the change in velocities, due to this effect is still less than 3%, the corrections, nonetheless have been incorporated in order to increase the overall accuracy.

CHAPTER 4

4.0 RESULTS AND DISCUSSION

A wide range of propellers, spanning the diameter range stated in the goals have been tested to date, and a number of runs have been completed with more propellers being constantly added to the inventory. Since all the results cannot be shown here, only a few representative results have been shown for the purpose of illustration. A website is currently being developed, and will host propeller performance data for propellers being tested at this facility using IPTS. Follow-on publications are also planed for future.

4.1 System and Procedure Validation

The first few test runs were aimed towards testing the measurement systems accuracy, verifying its repeatability and checking the overall data quality.

To establish confidence in procedure, first few experiments were designed similar to those conducted by Asson [6], [7]. Information needed for this purpose, such as tunnel-q, and data points collected, were backed out from performance plots in Asson's thesis [7]. Asson conducted his test runs at fairly low tunnel-q's and the RPM was also limited to 3,000, as his apparatus had vibrational issues. The propellers used here were the 14-4, 14-6 and the 16-6 propellers belonging to the Zinger family.

The comparative results with Asson's run for the Zinger 16-6 propeller are shown in Figure 6 below.

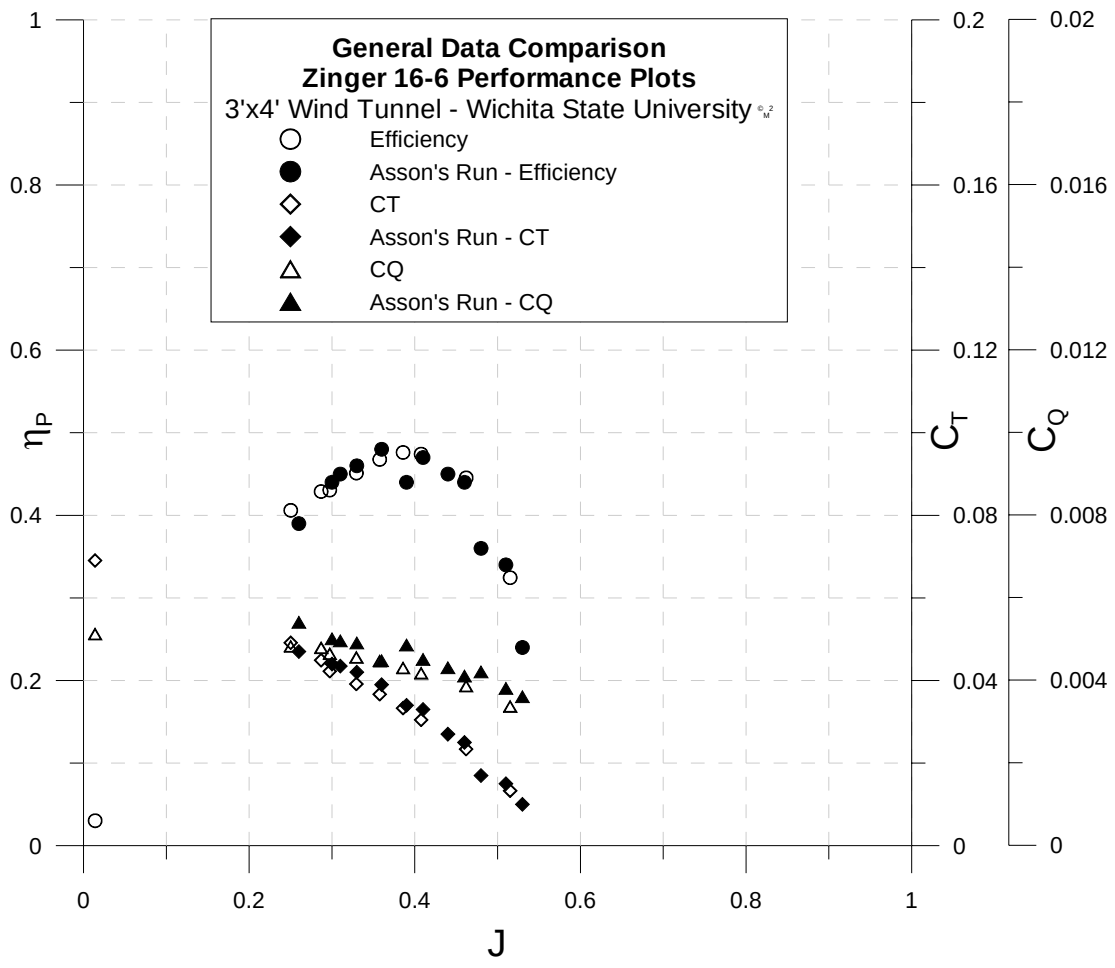

Figure 6: IPTS result comparison with Asson's data [7]

As can be observed in Figure 6, data collected by the Integrated Propulsion Test System matches that of Asson's experiment [7]. Similar results were observed for the other propellers.

One important point that should be noted here is that all these runs were conducted at very low RPM, forward velocities (or low q's) and Reynolds numbers range around 100,000 in order to match Asson's run conditions [6]. The flow in the test section at speeds around 40 ft/s (Tunnel q approximately 1.9

lb/ft^2), is relatively unsteady, not to mention the propeller being operated at less than half of its expected RPM, decreases the applied loads considerably, thereby increasing the variation in data.

4.2 System Sensitivity

Once the runs form Asson's thesis [6] were successfully duplicated, the apparatus sensitivity to tunnel flow was checked. As mentioned in the previous section this also helped check the flow quality in the tunnel's test section. This test was performed by comparing a baseline run (0° α and β) to runs at ±3° in α and β respectively. The results in terms of C_Q and C_T versus J are shown in Figures 7 and 8 below.

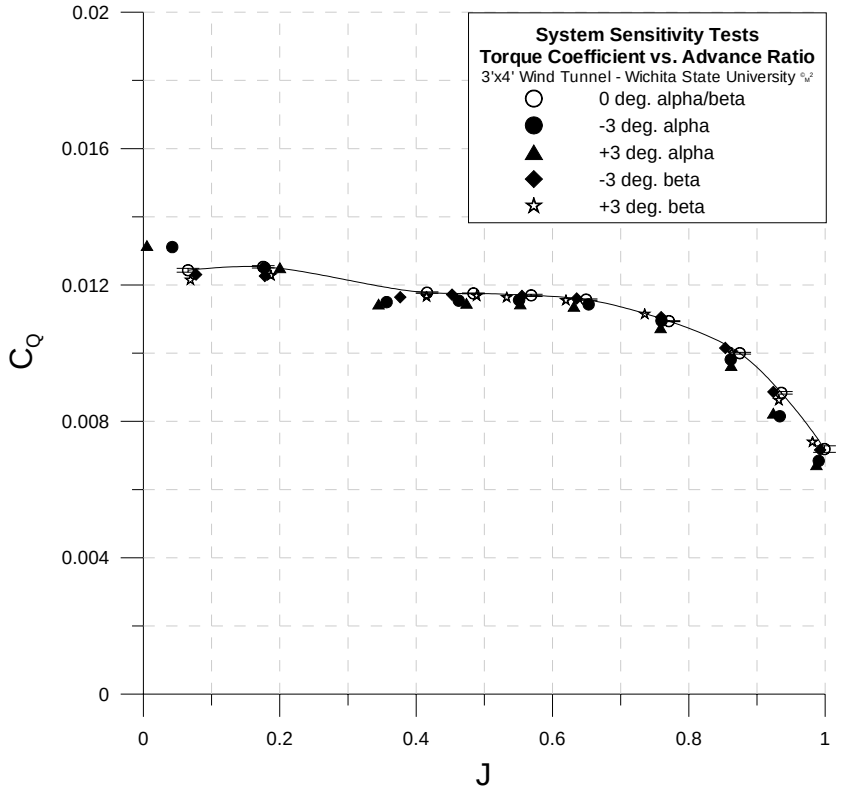

Figure 7: α and β sweep plots of C_Q vs. J

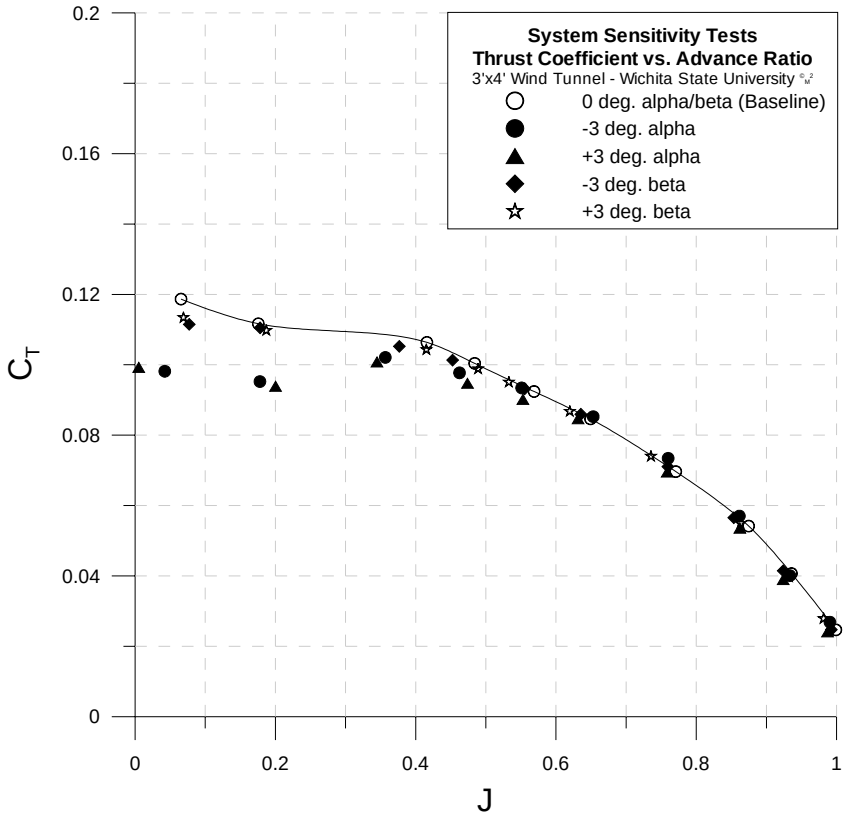

Figure 8: α and β sweep plots of C_T vs. J

As can be observed from Figures 7 and 8, torque sensitivity to the propeller disc plane orientation in any direction (α or β) is lower compared to the thrust sensitivity, which is higher in α compared to β.

However, the fact that the results for both +3° and –3° match for both α and β sweeps, suggests that the flow angularity present in the tunnel test section, is negligible.

4.3 Data Quality and Repeatability

The next tests on the agenda were aimed at building confidence in data by demonstrating the Integrated Propulsion Test System's ability to provide high quality repeatable data.

It should be noted here that repeat runs are performed for all propellers that are tested here, and are conducted on different days.

Figure 9 shows the performance data for two separate runs conducted for the 3-Blade, Master Air Screw 16-8 propeller. Efficiency, η_P is plotted along with C_Q, C_T and C_P as a function of J.

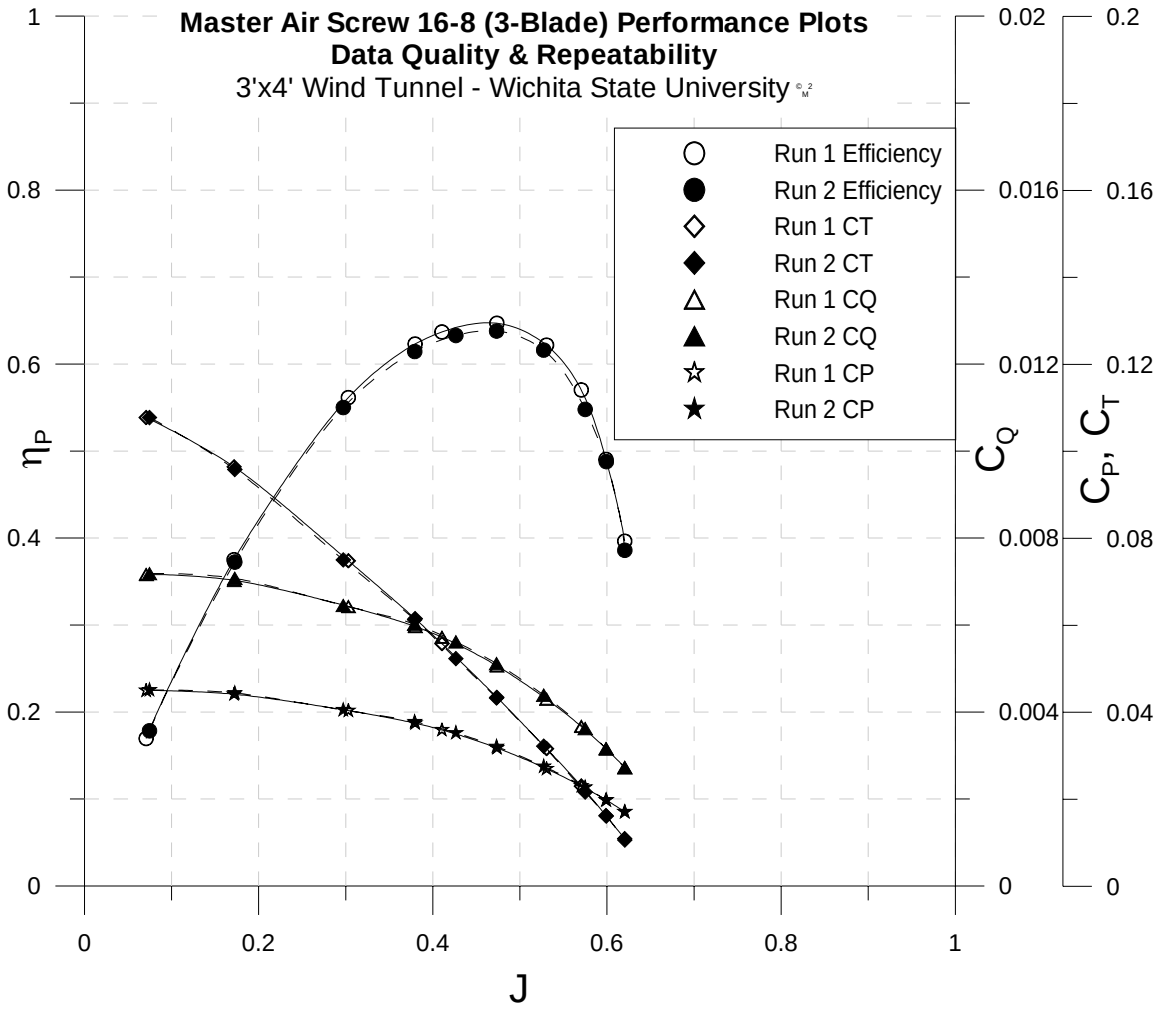

Figure 9: Sample plot 1 illustrating data quality and repeatability

The data for two runs, conducted on two different days compared well to the other. Similar trends can be observed in Figure 10, which charts propeller efficiency for the APC 12-12 E propeller measured on four different days. As can be observed in Figure 10, the data points repeat the efficiency curve with minimal scatter. A few different, randomly selected propellers were put through similar tests, and, a high repeatability was observed in all.

For the purpose of illustration two examples have been included in this thesis to show the data quality and repeatability as obtained through IPTS. Almost all comparisons demonstrate this capability of IPTS.

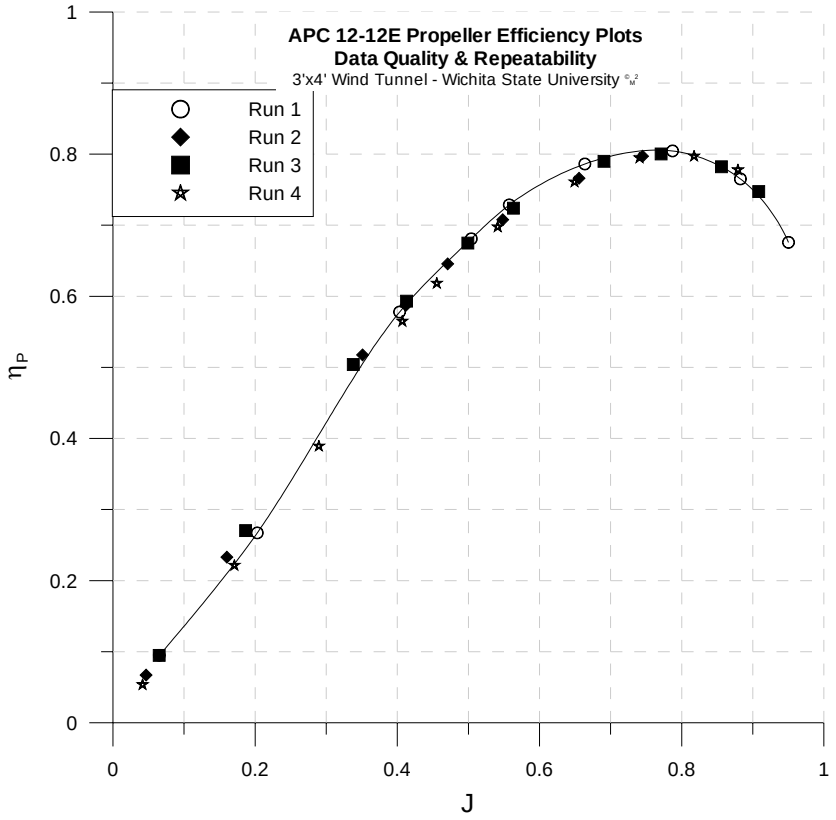

Figure 10: Sample plot 2 illustrating data quality and repeatability

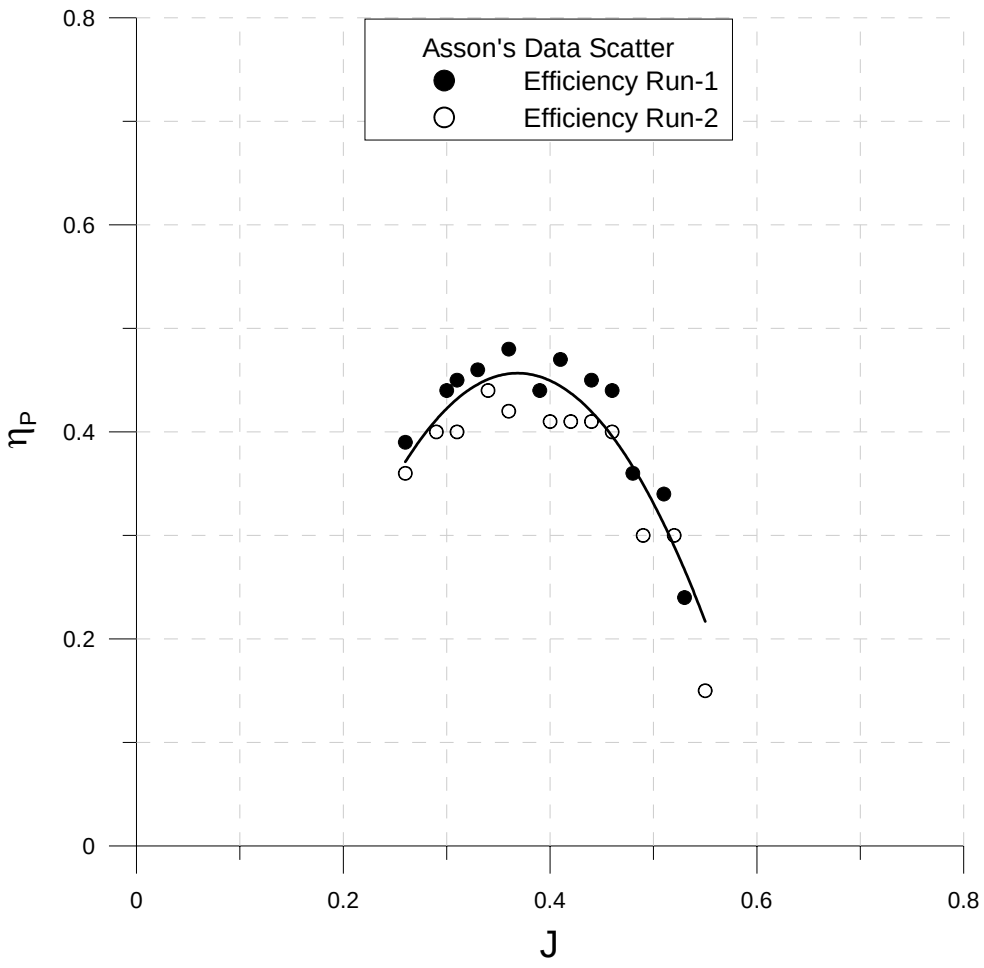

Figure 11: Plot illustrating scatter in Asson's data [7]

For the purposes of comparison, repeat run results obtained by Asson [7] have also been shown in Figure 11, data points for which were obtained from Asson's thesis report [7]. The high scatter in his data can be attributed to the restrictions in the run conditions within which he had to operate, as imposed by his system.

4.4 Observations – Issues with propeller manufacturability

Certain limitation issues arising due to propeller manufacture quality were observed and have been demonstrated through the investigational test results described in this section. The limitation of IPTS as mentioned in the previous sections has only been the propeller diameter, which is only restricted due to the dimensions of test section. This section demonstrates some limitations, in terms of repeatability as imposed due to the propellers manufacturability.

It should be noted here that the Integrated Propulsion Test System is intended to measure performance of a given propeller. The accuracy of this system has also been demonstrated in as many ways as possible. Therefore, deviations in propeller performance plots are only attributed to physical variations in similar propellers due to poor manufacturability.

Comparison runs have been performed between two propellers made by the same manufacturer. This test has been designed with the point of exploring the manufacturer's product reliability and the variance in manufacturability. For the purpose of comparison, contrasting results have been shown in Figures 12 and 13, where two propeller sets, each set having the same geometry, from two different manufacturers, are compared.

As can be observed that form Figures 12 and 13, there is a distinct variation in propeller performance in Figure 12, especially in the efficiency and thrust coefficient, compared to a very minor variation in propeller data as in Figure 13.

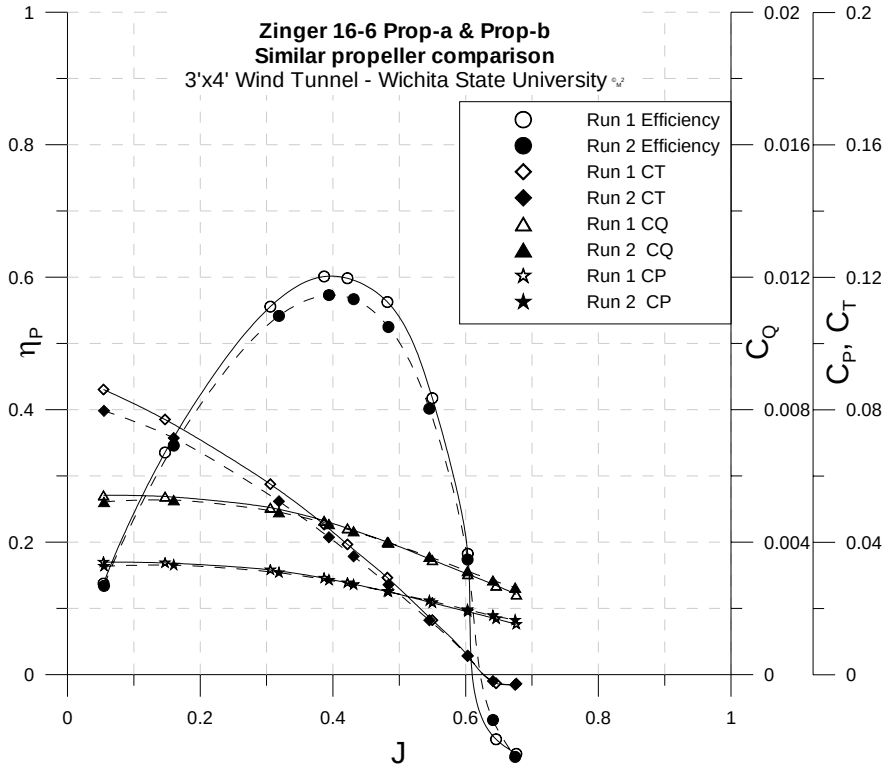

Figure 12: Example plot illustrating high performance variation

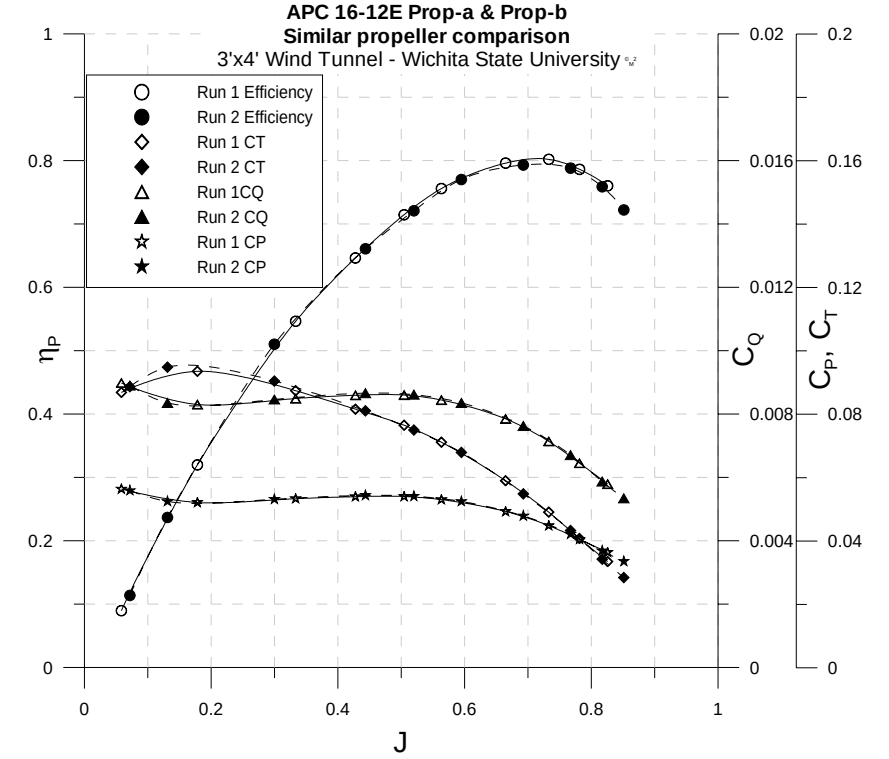

Figure 13: Example plot illustrating low performance variation

All the tests discussed above helped verify the setup, procedure and establish confidence in the quality of data being collected. Hereafter, the data from the propellers tested are being archived in an electronic database.

4.5 Sample Output File

The data acquisition and reduction program, as mentioned previously, directly outputs four performance plots of η_P, C_Q, C_T and C_P as function of J and a summary table, per test, as shown in Figure 14 and Table 3.

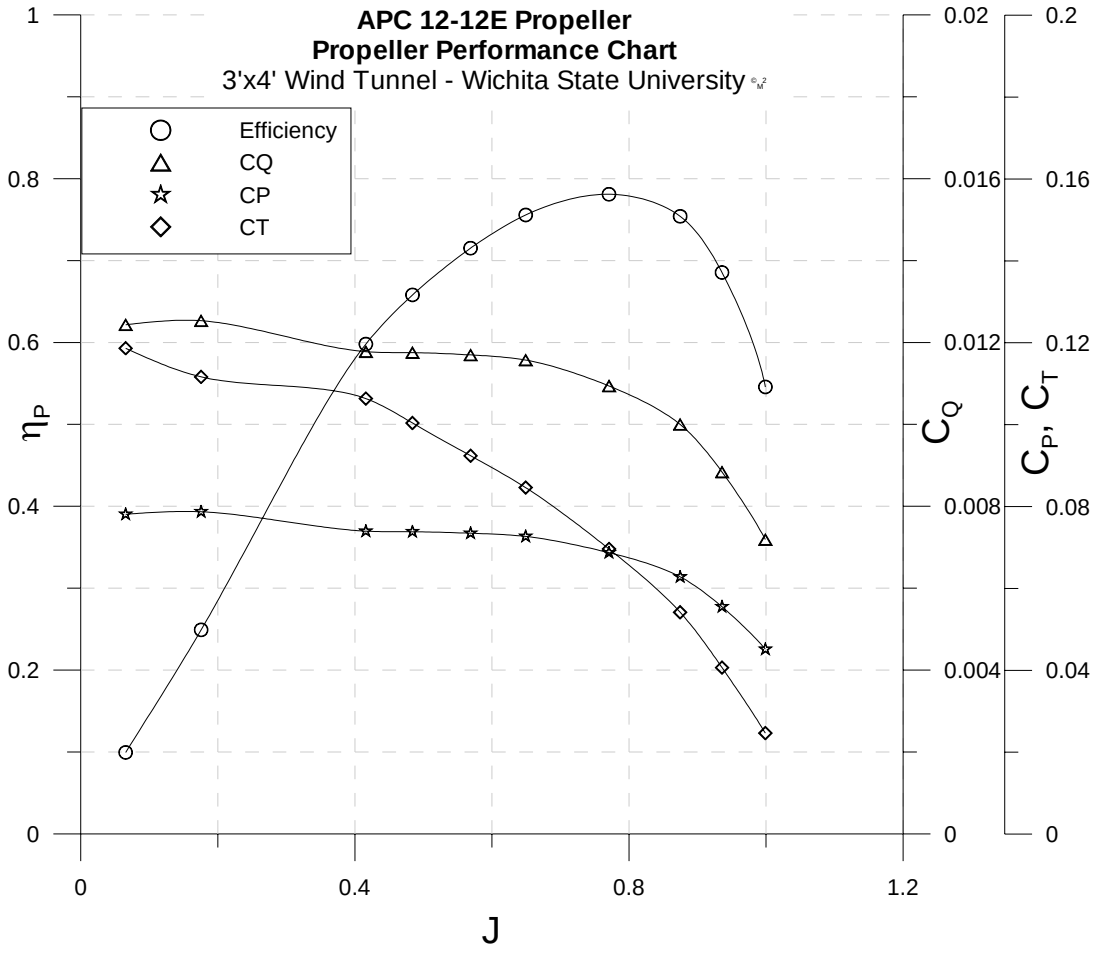

Figure 14: Data reduction program sample output plot

TABLE 3: DATA REDUCTION PROGRAM SAMPLE OUTPUT TABLE

SUMMARY					
PROP	EAPC	DIA	12	PITCH	12
	q(psf)	U (ft/s)	T (lb)	Q (in-lb)	RPM
	0.07	6.90	3.10	3.90	6,323
	0.42	17.95	2.75	3.70	6,131
	2.32	43.71	2.77	3.67	6,304
	3.25	51.89	2.72	3.82	6,431
	4.41	60.65	2.47	3.76	6,398
	5.78	69.60	2.29	3.76	6,431
	8.37	83.92	1.94	3.67	6,533
	11.10	96.82	1.56	3.46	6,641
	13.42	106.56	1.24	3.24	6,833
	16.35	117.70	0.81	2.82	7,069
J	η_P	C_T	C_P	C_Q	$Re_{0.75}$
0.07	0.10	0.1187	0.0781	0.0124	90,370
0.18	0.25	0.1117	0.0787	0.0125	87,860
0.42	0.60	0.1064	0.0740	0.0118	91,495
0.48	0.66	0.1004	0.0738	0.0118	93,845
0.57	0.72	0.0924	0.0735	0.0117	94,069
0.65	0.76	0.0846	0.0727	0.0116	95,349
0.77	0.78	0.0696	0.0687	0.0109	98,233
0.87	0.75	0.0542	0.0628	0.0100	101,239
0.94	0.69	0.0407	0.0555	0.0088	105,054
1.00	0.55	0.0247	0.0452	0.0072	109,706

4.6 Some Selected Results

For the purpose of illustration, performance plots of a few randomly selected propellers, spanning the diameter range covered under this project, are shown in Figures 15, 16, 17 and 18 below.

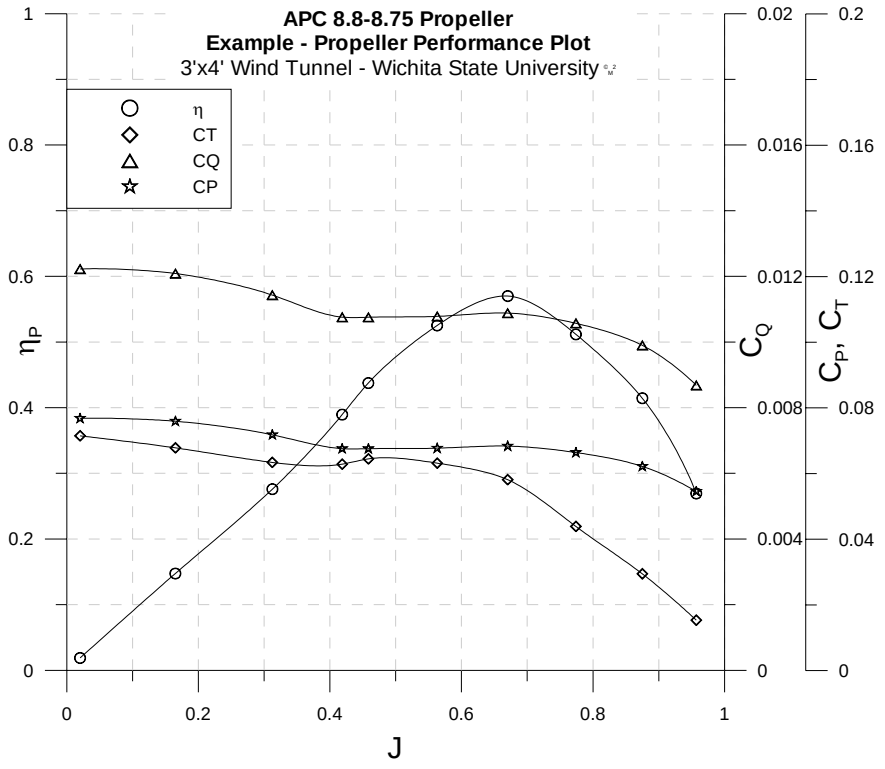

Figure 15: Sample performance plot for APC 8.8 – 7.5 Propeller

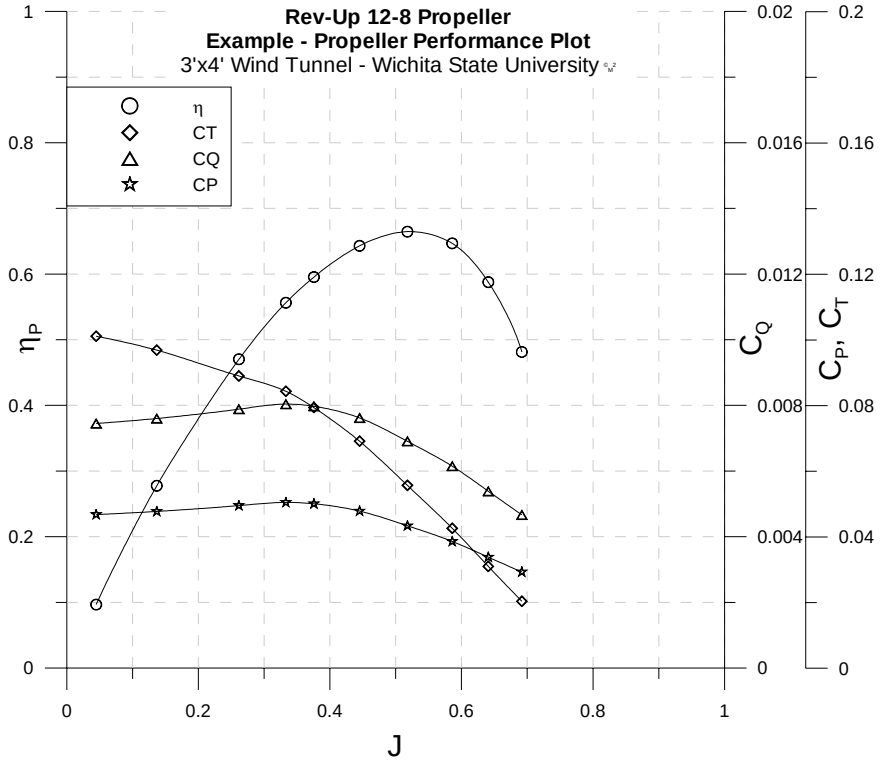

Figure 16: Sample performance plot for Rev-Up 12 – 8 Propeller

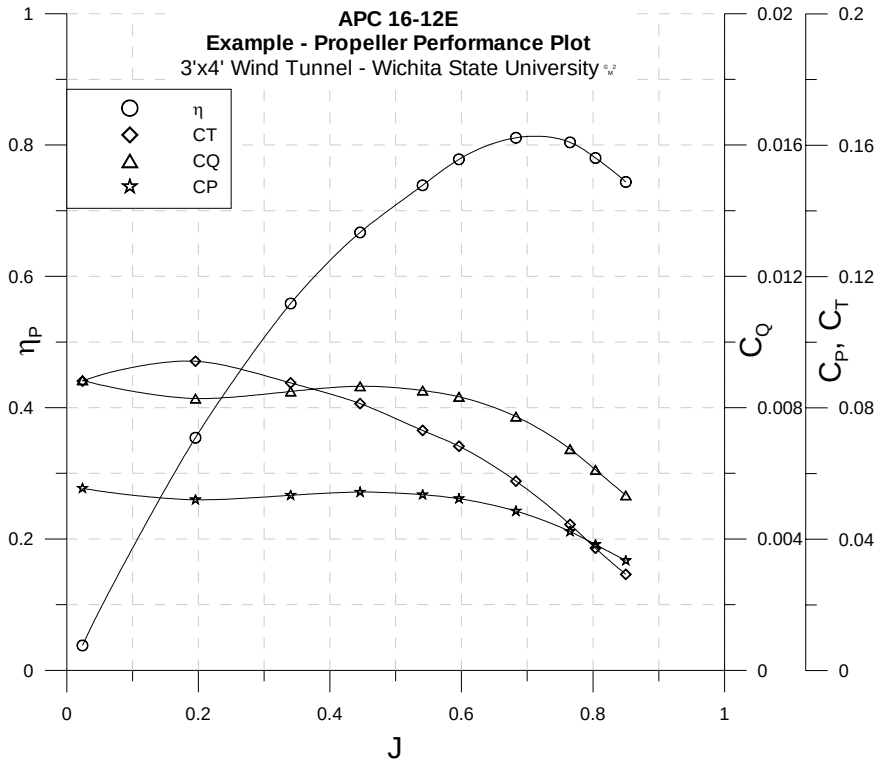

Figure 17: Sample performance plot for APC 16 – 12 E Propeller

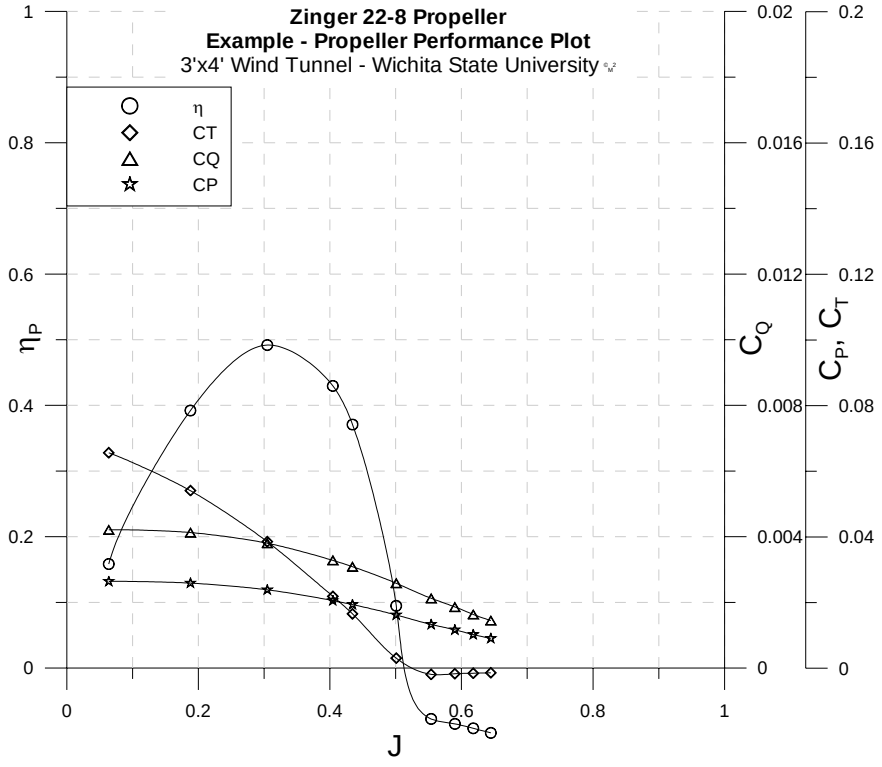

Figure 18: Sample performance plot for Zinger 22 – 8 Propeller

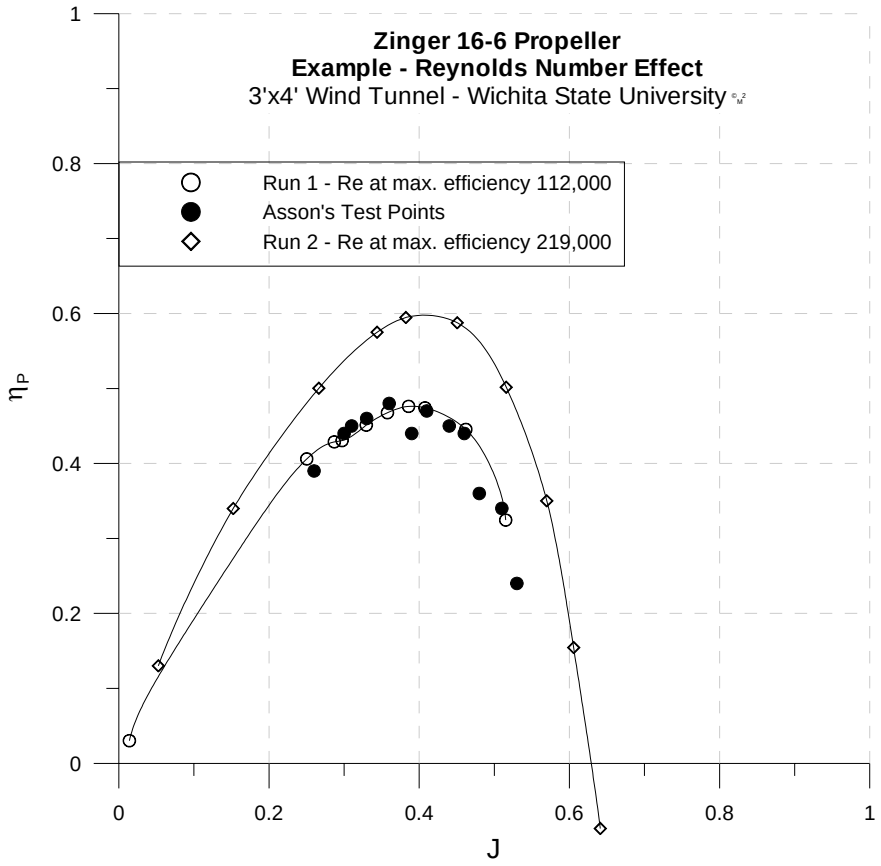

Figure 19: Sample plot illustrating Reynolds number effect

4.6 Observation and Discussion

To this date over 60 propellers have been tested and their performance mapped. More propellers are being added to this list on a regular basis. Less than 0.1% variation has been generally observed in data collected from all propellers tested using the Integrated Propulsion Test System. The system, as mentioned previously, is very well behaved. The root mean squared uncertainties observed during calibration and check load processes were 0.0095% in thrust and 0.0039% in torque. Since the uncertainties in the coefficients are dependent on the particular propeller and the advance ratio, their values have been included

in the table provided along with the propeller performance charts. These however were 0.2% in C_T and C_P and, 0.15% in C_Q for the worst case scenario. Since these values depended on the measurement taken from each instrument, they varied for each propeller and each data point recorded. Typical values for these uncertainties, as observed, were 0.05% in C_T and C_Q and 0.003% in C_P.

Also, as mentioned earlier, the other important observation made was that the scatter in repeat run data increased as Reynolds number were decreased by spinning the propellers below 3000 RPM at tunnel speeds of less than 50 ft/s. As an interesting note, Low Reynolds number effects on propeller performance curves have been observed (Figure 19). Since the Reynolds number at any given point during a run would differ due to increasing tunnel speeds, the low Reynolds number effect was studied by comparing the Reynolds number (chord length at $3/4^{th}$ radius location) that occurred at maximum efficiency for a particular propeller.

Although, examples for only a few representative propellers have been shown in this thesis, a website is currently being setup where data for more propellers will be made available to public.

4.6.1 A brief note on Performance calculators

The experimental results were also compared to results from performance calculator programs available in the public domain, such as PropSelector [17]. The results, as expected, did not match and neither did it show any consistent trends. The reason for this could not be verified since, no source code or the

information on the analytical method used by PropSelector [17], is available. Thus, since the credibility of this program is questionable, results obtained from this have been ignored.

Program based on the Combined Blade Element and Momentum Theory [2], although fairly accurate, could not be used here. This program requires users to input airfoil data and propeller geometry information such as twist distribution. Such information is generally not made available to the end user by the propeller manufacturer. Furthermore, propellers such as those tested here, do not use standard airfoils. Most of the time, the airfoils used herein are flat bottomed or modified airfoils, and obtaining lift curve slope for such airfoils becomes very difficult. Hence, experimental results could not be compared to this program either.

CHAPTER 5

5.0 CONCLUSIONS

The results from all the tests performed so far have been very encouraging. All expectations from this exercise have been surpassed and the following conclusions have been drawn based on the results obtained and the observations made herein.

- The results of Propeller performance experiments conducted by Asson in his thesis [6] have been successfully repeated and matched, as described in the System and Procedure Validation section.
- The sensitivity and repeatability studies and tests show that the system is highly repeatable with minimal scatter in data.
- The apparatus has remained structurally sturdy at high motor RPM and high Tunnel-q, not affecting the data quality and repeatability, a common problem faced by previous investigators.
- Typical uncertainties in the non-dimensional performance coefficients, C_T and C_Q are 0.05% and 0.003% for C_P.
- Low uncertainty in all measured variables in all tests increases the confidence in data and demonstrates high measurement system and tunnel flow quality.

Thus it can be concluded that the primary goal of this effort has been successfully accomplished and expectations been exceeded.

With over 30 unique propellers tested and over 150 runs logged, a reliable propeller performance database has been created, with more propellers being tested and data being added on a regular basis.

A website is currently being setup for the public to access the propeller performance database.

The tests conducted so far have also demonstrated the systems design time efficiency. Entire experiment can be completed within ten to fifteen minutes and, the ability to quickly change propellers, greatly reduces the wind tunnel occupancy time, which can prove very valuable.

Moreover, this system will be a valuable experimental tool for investigators to not only measure and determine propeller experimentally, but will also help designers gain an insight needed to further improve or optimize an existing propeller or a new propeller.

CHAPTER 6

6.0 RECOMMENDATIONS

Substantial amount of time and effort has been spent in the development of this apparatus and the experimental procedure. Extensive work has been performed to fine tune the system as much as possible to increase its data output accuracy. However, a few recommendations that can further improve this system are:

- Incorporate power measurement and control into the data acquisition and reduction routine. This would help further automate the process and eliminate the manual task of logging current and voltage data associated with this experiment. Although, it should be noted here that power being supplied to the motor is in no way associated with any propeller performance parameters, but can be helpful in future if motor and system performance too, were to be calculated.
- Design and build a ‘universal’ motor adapter with a smaller frontal area. This would help accommodate a smaller diameter couling, reducing the overall frontal area.

As far as the experiments are concerned, this system can be used with little or no modifications to investigate a wide range of subjects relating to rotary wings. However, since Low Reynolds number effects have been observed here,

further investigation of this effect is recommended, since this may lead to correction charts or tables to compensate for such effects.

The Integrated Propulsion Test System is a valuable asset and addition to the 3’ x 4’ Low Speed Wind Tunnel’s already present high quality force and pressure measurement systems, increasing the bandwidth of experiments that can be reliably performed.

LIST OF REFERENCES

LIST OF REFERENCES

[1] Boucher, B., Electric Motor Handbook, 3rd Print, 2001, Chaps. 1, 2, 9.

[2] Seddon, J. and Newman, S., Basic Helicopter Aerodynamics, 2nd ed., AIAA Education Series, VA, 2001, Chaps. 2, 3.

[3] APC Propellers, URL: http://www.apcprop.com/Engineering/engineering_design.html [cited 6 May 2005].

[4] Bass, R. M., 'Techniques of Model Propeller Testing," SAE Paper 83-0750, April 1983.

[5] Stefko, G. L., Bober, L. J. and Neumann, H. E., "New Test Techniques and Analytical Procedures for Understanding the Behavior of Advanced Propellers," SAE Paper 83-0729, April 1983.

[6] Asson, K. M. and Dunn, P. F., "Compact Dynamometer System that can Accurately Determine Propeller Performance," Journal of Aircraft, Vol. 29, No. 1, 1992, pp. 8-9.

[7] Asson, K. M., "The Development of an Advanced Dynamometer System to Experimentally Determine Propeller Performance," M.S. Thesis, University of Notre Dame, Notre Dame, IN, 1990.

[8] Bass, R. M., "Small Scale Wind Tunnel Testing of Model Propellers," 24th Aerospace Sciences Meeting, AIAA-86-0392, January 1986.

[9] Molland, A. F. and Turnock, S. R., "A Propeller Thrust and Torque Dynamometer for Wind Tunnel Models," Strain, Blackwell Sciences Ltd., Vol. 38, 2002, pp. 3-10.

[10] MH-Aerotools, URL: http://www.mh-aerotools.de/airfoils/pylonprops_1.htm [cited 7 November, 2005].

[11] Wikipedia – Online Encyclopedia, URL: http://en.wikipedia.org/wiki/Model_aircraft [cited 7 November, 2005].

[12] Kline, S. J. and McClintok, F. A., "Describing Uncertainties in Single Sample Experiment," Mechanical Engineering, Vol. 75, No. 1, 1953, pp. 3-9.

[13] Holman, J. P., Experimental Methods for Engineers, 6th ed., McGraw Hill, New York, 1994, Chaps. 3.

[14] Pope A., Wind Tunnel Testing, 2nd ed., John Wiley, New York, 1954, Chaps. 6.

[15] Raymer, D. P., Aircraft Design: A Conceptual Approach, 3rd ed., AIAA Education Series, VA, 2001, Chap. 13.

[16] Glauert, H., Wind Tunnel Interference on Wings, Bodies, and Air-screws, R&M 1566, 1933.

[17] Propeller Selector program (freeware) PropSelector, URL: http://www.gylesaero.com/freeware/propcalc.shtml [cited 7 November, 2005].

[18] Henry V. Borst," Aerodynamic Design and Analysis of Propellers for Mini-Remotely Piloted Air Vehicles", USAAMRDL-TR-77-45A, Volume-I, January 1978.

[19] Henry V. Borst," Summary of Propeller Design Procedures and Data", USAAMRDL-TR-73-34A, Volume-I, January 1973.